JACC: CARDIOVASCULAR IMAGING
VOL. 8, NO. 4, 2015

ISSN 1936-878X/$36.00
PUBLISHED BY ELSEVIER INC.
http://dx.doi.org/10.1016/j.jcmg.2014.10.015

Accuracy of OCT, Grayscale IVUS, and Their Combination for the Diagnosis of Coronary TCFA

An Ex Vivo Validation Study

Kenichi Fujii, MD,* Hiroyuki Hao, MD,† Masahiko Shibuya, MD,* Takahiro Imanaka, MD,* Masashi Fukunaga, MD,* Kojiro Miki, MD,* Hiroto Tamaru, MD,* Hisashi Sawada, MD,* Yoshiro Naito, MD,* Mitsumasa Ohyanagi, MD,‡ Seiichi Hirota, MD,† Tohru Masuyama, MD*

ABSTRACT

OBJECTIVES This study sought to assess the accuracy of optical coherence tomography (OCT), gray-scale intravascular ultrasound (IVUS), and their combination for detecting thin-cap fibroatheromas (TCFA).

BACKGROUND The extent to which the imaging characteristics of OCT and IVUS correlate with histologically defined TCFA is unknown.

METHODS IVUS and OCT examinations identified focal plaques in 165 coronary arteries from 60 autopsy hearts. A total of 685 pairs of images of OCT and IVUS were compared with histology. By OCT, a TCFA was defined as a signal-poor region with diffuse borders and cap thickness <65 μm. By IVUS, a TCFA was defined by the presence of echolucent zones and/or ultrasound attenuation in areas of positive remodeling. By histology, 12 of 685 focal plaques were classified as TCFAs.

RESULTS With histology as the gold standard, the sensitivity, specificity, positive predictive value, negative predictive value, and overall diagnostic accuracy for OCT-derived TCFA were 100%, 97%, 41%, 100%, and 98%, respectively. The corresponding numbers for IVUS-derived TCFA were 92%, 93%, 19%, 99%, and 93%, respectively. The histological findings underlying the false positive diagnoses of OCT for TCFA included large amounts of foam cell accumulation on the luminal surface, large amounts of microcalcifications at the surface, large amounts of hemosiderin accumulation, or organized thrombus. In contrast, histological causes of mischaracterization of TCFA by IVUS were mostly TCFA. When both OCT and IVUS criteria for TCFA were required to be met, the sensitivity, specificity, positive predictive value, negative predictive value, and overall diagnostic accuracy were 92%, 99%, 69%, 99%, and 99%, respectively.

CONCLUSIONS In the present study, neither OCT nor IVUS were optimal to detect TCFA. The combined use of OCT and IVUS may improve TCFA detection accuracy. (J Am Coll Cardiol Img 2015;8:451–60) © 2015 by the American College of Cardiology Foundation.

Acute coronary syndromes (ACSs) cause considerable immediate morbidity and mortality and are associated with a high risk of additional coronary events within a year (1). The most common cause of these acute coronary events is atherosclerotic plaque rupture followed by thrombus formation (2). Postmortem studies have shown that the precursors of the ruptured plaque, known as thin-cap fibroatheromas (TCFAs), have certain characteristics: a thin fibrous cap

From the *Cardiovascular Division, Hyogo College of Medicine, Nishinomiya, Japan; †Department of Surgical Pathology, Hyogo College of Medicine, Nishinomiya, Hyogo, Japan; and the ‡Division of Coronary Heart Disease, Hyogo College of Medicine, Nishinomiya, Japan. The authors have reported that they have no relationships relevant to the contents of this paper to disclose.

Manuscript received June 13, 2014; revised manuscript received September 30, 2014, accepted October 3, 2014.

ABBREVIATIONS AND ACRONYMS

ACS = acute coronary syndrome

DA = overall diagnostic accuracy

IVUS = intravascular ultrasound

NPV = negative predictive value

OCT = optical coherence tomography

PPV = positive predictive value

TCFA = thin-cap fibroatheroma

(<65 μm), a large necrotic core, and increased macrophage activity (1,3). The identification of the thin fibrous cap is important because plaque is prone to rupture when the thickness of the fibrous cap becomes <65 μm (2,3).

Intravascular ultrasound (IVUS) is one method to characterize plaque composition and potentially provides insights into the features of vulnerable plaques. Previous IVUS studies indicated that the features associated with plaque vulnerability include an eccentric pattern, presence of an echolucent zone (4), plaque with ultrasound attenuation (5), and presence of thrombi (6). However, IVUS at frequencies in the 20 to 40 MHz range has an axial resolution of 150 to 200 μm and a lateral resolution of 250 μm (7). Optical coherence tomography (OCT) has been introduced recently as a high-resolution imaging method (8). TCFAs defined by OCT are found more commonly in patients with ACS than in those with stable coronary artery disease (9). However, the major limitation of OCT is poor tissue penetration. Thus, the vessel-remodeling status, which is one of the main findings via IVUS for plaque vulnerability, cannot be evaluated. This study investigated modalities to detect TCFAs by examining the accuracy of OCT, gray-scale IVUS and their combination compared to histological images.

METHODS

SPECIMENS. A total of 165 coronary arteries from 60 cadavers were examined to compare combined OCT and IVUS images and histological images. In all patients, the cause of death was noncardiac death. One patient had symptomatic cardiovascular disease, and another patient had a history of myocardial infarction. All coronary arteries were dissected at autopsy within 6 h after death. The harvested coronary arteries were stored immediately in phosphate-buffered saline. The time between death and OCT and IVUS examinations did not exceed 12 h. The experimental protocol was approved by the Institutional Review Board of Hyogo College of Medicine. The ex vivo study protocol was also approved by the Institutional Review Board of Hyogo College of Medicine, and written informed consent was obtained from patients' relatives in all cases.

STUDY PROTOCOL. At autopsy within 6 h after death, the coronary arteries with plaques were dissected along with surrounding fatty tissue for the ex vivo imaging of OCT and IVUS in 0.9% saline at a temperature of 37°C. The surrounding fatty tissue was carefully dissected from each coronary specimen. Thereafter, side branches were tied off to preserve the perfusion pressure of 60 to 80 mm Hg. Conventional grayscale IVUS examinations were conducted to identify the lesions' mild to severe plaque accumulation using a commercially available 40-MHz IVUS catheter (Terumo Corp., Tokyo, Japan). The plaque burdens, which were calculated as plaque and media area divided by vessel area, of 50% or more were considered to be lesions with mild to severe plaque accumulation. After the IVUS imaging, the OCT examinations were performed on each mild to severe plaque accumulation to assess the lesion's morphology. In the present study, a time-domain OCT system (Image Wire, LightLab Imaging, Westford, Massachusetts) was used because the position of the interrogating beam on the specimen can be monitored by a visible-light beam in real time (**Figure 1**). After the IVUS and OCT examinations, a 6-0 Prolene (Ethicon, Somerville, New Jersey) suture with a tapered surgical needle was inserted into each lesion on the specimen under the direction of a visible red light.

OCT AND IVUS IMAGING AND ANALYSIS. OCT images were analyzed using proprietary software (LightLab Imaging) by 2 independent observers who were blinded to the histological diagnosis and using validated criteria for plaque characterization (10). For all plaques with an OCT-determined lipid core, the fibrous cap thickness was measured. The cap thickness at its thinnest point over the entire lesion was measured 5 times at its visibly most thin position, and the average of the 3 middle values was computed to minimize an error of measurement. The size of a lipid lesion was quantified according to the arc of the lipid tissue as it appeared in quadrants of the cross-sectional OCT image. For OCT analysis, we defined an OCT-derived TCFA as a plaque with lipid content in >1 quadrant with a fibrous cap measuring <65 μm (11).

Quantitative IVUS measurements were performed at the sections with minimum lumen area, as well as at the proximal reference segments, which were defined as the most normal-looking cross sections (largest lumen with smallest plaque and media) within the same arterial segment (typically, <10 mm proximal to the lesion) but before any large side branch. Using planimetry software (Echoplaque2, INDEC Systems, Mountain View, California), we traced and measured the vessel and lumen area. A remodeling index was calculated as the vessel area at the section with minimum lumen area divided by

FIGURE 1 Approach to Achieve Optimal Coregistration of the Optical Coherence Tomography Image With the Histological Image

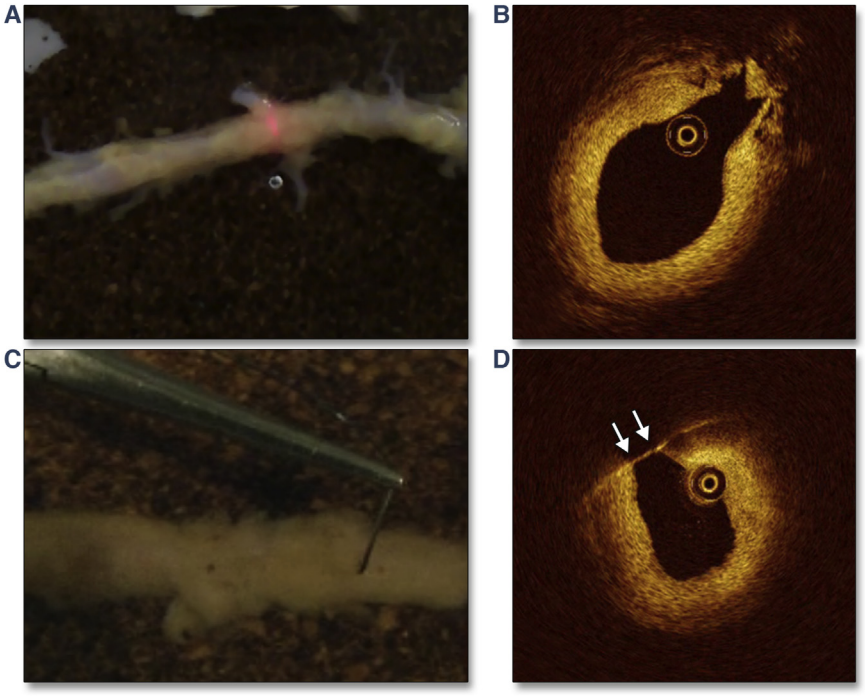

(A) Optical coherence tomography (OCT) examination after careful dissection of the surrounding fatty tissue from coronary specimen. The position of the interrogating beam on the specimen can be monitored by a visible light beam in real time. **(B)** A corresponding OCT image indicating a cross section with bifurcation. **(C)** Insertion of a 6-0 Prolene suture with a tapered surgical needle into the coronary specimen as a mark under the direction of visible light. **(D)** A corresponding OCT image containing a surgical needle **(arrows)**.

the proximal reference vessel area. Qualitative IVUS analyses were performed using a published definition (12). Lesion plaque composition was assessed visually according to the American College of Cardiology Clinical Expert Consensus Document on Standards for Acquisition, Measurement, and Reporting of Intravascular Ultrasound Studies (12). Plaque with ultrasound attenuation was defined as an IVUS finding with backward signal attenuation behind a plaque without dense calcium. The arc of ultrasound attenuation was measured in degrees with a protractor centered on the lumen (13). A lipid pool-like image was defined as a pooling of low-echoic material or echolucent material covered with a high-echoic layer (14). We defined a grayscale IVUS-derived TCFA-like image as a lesion meeting all the following 3 criteria: 1) the presence of $>180^\circ$ of ultrasound attenuation without dense calcium (13) or $>90^\circ$ of lipid pool-like images in at least five consecutive frames; 2) a remodeling index of >1.0; and 3) a plaque burden of ≥50%.

HISTOLOGICAL STUDY. Each coronary arterial section was examined to compare OCT, grayscale IVUS, and histological diagnoses. Subsequently, 48 h after fixation with 10% buffered formalin, ring-like arterial specimens obtained at a same level as the imaging study were decalcified for 5 h and then were embedded in paraffin and cut in 4-μm transverse sections perpendicular to the longitudinal axis of the artery. They were stained with hematoxylin-eosin, elastic van Gieson stain, and Masson's trichrome. TCFA was defined as a lesion containing a necrotic core covered by a thin (<65 μm) fibrous cap (2). These histological classifications were on the basis of the evaluation of a single pathologist (H.H.) who was blinded to the imaging results.

STATISTICS. Data are presented as frequencies or mean ± 1 SD. The accuracy of grayscale IVUS and OCT for the characterization of TCFA was analyzed by application of grayscale IVUS and OCT criteria to the validation set, and histopathological consensus diagnosis was definitive. Intraobserver

and interobserver variability were quantified using κ concordance analysis for OCT and IVUS plaque characterization.

RESULTS

In 60 hearts, 165 coronary arteries were dissected and imaged with grayscale IVUS and OCT. The average length of all coronary arteries sectioned was 83.7 ± 23.0 mm in the left anterior descending artery, 67.9 ± 15.8 mm in the left circumflex artery, and 114.7 ± 37.9 mm in the right coronary artery. We identified 685 focal plaques that displayed mild to severe accumulation in 141 diseased arteries. Of those, only 12 plaques (2%) were classified as TCFAs by histological analysis.

A summary of the lesion diagnoses is shown in Figure 2. Of 685 plaques, OCT examination diagnosed 29 plaques (4%) as TCFA, and grayscale IVUS analyses identified 58 plaques (8%) as grayscale IVUS-derived TCFA-like images. Intraobserver variability yielded acceptable concordance for grayscale IVUS-derived TCFA-like images (κ = 0.84) and OCT-diagnosed TCFA (κ = 0.92). Interobserver variability showed slightly lower concordance for grayscale IVUS-derived TCFA-like images (κ = 0.76) and OCT-derived TCFA (κ = 0.81).

ACCURACY OF OCT TO DIAGNOSE HISTOLOGICAL TCFA. Figure 3A shows the diagnostic accuracies of OCT for TCFA. Of 29 OCT-derived TCFA, only 12 plaques (41%) were classified as TCFAs by histological analysis. The sensitivity, specificity, positive predictive value (PPV), negative predictive value (NPV), and overall diagnostic accuracy (DA) of OCT for characterizing TCFA using histology as a standard were 100%, 97%, 41%, 100%, and 98%, respectively (Figure 3B). The histological findings underlying the false positive diagnoses of OCT for TCFA included: 1) large amounts of foam cell accumulation on the luminal surface (n = 7); 2) large amounts of microcalcifications at the surface of the fibrous intima (n = 7); 3) large amounts of hemosiderin accumulation on the luminal surface (n = 2); or 4) organized thrombus (n = 1) (Figure 4). No false negative diagnoses of OCT for TCFA were apparent in the current analysis.

ACCURACY OF COMBINED OCT AND IVUS TO DIAGNOSE HISTOLOGICAL TCFA. Only 16 plaques (2%) met both criteria for both OCT-derived and grayscale IVUS-derived TCFA-like images (Figure 5). PPV increased from 41% to 69% when IVUS was used in combination with OCT. The sensitivity, specificity, PPV, NPV, and DA of the combined use of OCT and IVUS for characterizing TCFA using histology as a standard were 92%, 99%, 69%, 99%, and 99%, respectively (Figure 3C). Only 1 histological TCFA was not diagnosed as an OCT and IVUS defined TCFA by combined use of OCT and IVUS. Although OCT produced an image with the appearance of TCFA, the image did not meet the criteria for a grayscale IVUS-derived TCFA-like image because the vessel size at the site with minimum lumen area was smaller than the proximal reference vessel area (negative remodeling).

ACCURACY OF IVUS TO DIAGNOSE HISTOLOGICAL TCFA. Figure 3A shows the diagnostic accuracies of grayscale IVUS-derived TCFA-like image. The sensitivity, specificity, PPV, NPV, and DA of grayscale IVUS for characterizing TCFA considering histology as a standard were 92%, 93%, 19%, 99%, and 93%, respectively. However, of these TCFA images diagnosed with grayscale IVUS, only 11 plaques met histological criteria for TCFA. Most grayscale IVUS-derived TCFA-like images that did not meet the histological criteria for TCFA were diagnosed as TCFAs by histological analysis (Figure 6).

DISCUSSION

Although OCT was somewhat more accurate than IVUS, neither OCT nor IVUS were perfectly accurate for detecting TCFA. With histology as the gold standard, most grayscale IVUS-derived TCFA-like images were diagnosed as TCFAs; and most false positive

FIGURE 2 Summary of Plaque Diagnosis

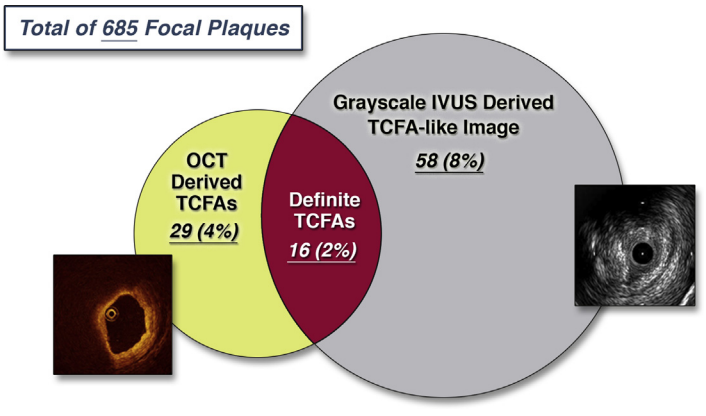

Among 685 mild to severe stenoses in 60 hearts, grayscale intravascular ultrasound (IVUS) diagnosed 58 lesions as grayscale IVUS-derived thin-cap fibroatheroma (TCFA)–like image (8%), and optical coherence tomography (OCT) revealed 29 lesions (4%) as OCT-derived TCFA. Sixteen lesions (2%) met the criteria of both grayscale IVUS-derived TCFA and OCT-derived TCFA and were diagnosed as OCT- and IVUS-defined TCFA.

diagnoses of OCT for TCFA contained large amounts of foam cell accumulations or microcalcification on the luminal surface.

Several IVUS studies have shown the association of positive arterial remodeling in ACS and angiographically complex lesions (15,16). Other IVUS features associated with plaque vulnerability may include the presence of an echolucent zone (17) and ultrasound attenuation (5). Plaque morphology with echolucent or signal-free zones within plaques has been associated with lipidic tissue accumulations (17). In addition, previous studies of human cadaver coronary arteries suggest that plaque with ultrasound attenuation may contain fibrolipidic tissue with a necrotic core (5). Therefore, the evaluation of plaque morphology by IVUS may help to identify vulnerable plaques.

The major limitation of IVUS is its insufficient spatial resolution. IVUS, at frequencies in the 20- to 40-MHz range, has an axial resolution of 150 to 200 μm. It is now widely recognized that TCFAs, which are characterized by a large necrotic core with an overlying thin fibrous cap measuring <65 μm, are the precursors of plaque ruptures (2). Although it can visualize deep structures, IVUS is not a suitable imaging modality for the detection of the thin fibrous caps that are a major feature of vulnerable plaques.

Because OCT measures the intensity of light returning from a tissue, tissues that have a higher heterogeneity in their optical index of refraction exhibit stronger optical scattering and therefore a stronger OCT signal. Thus, in OCT examination of atherosclerotic plaques, fibrous plaques present as homogeneous signal-rich regions with low attenuation because of elevated reflections from collagen fibers. In contrast, lipidic tissues appear as low-signal-intensity regions with diffuse borders because of multiple scattering in lipids at light wavelengths around 1,000 nm (18). Previous histopathological validation studies reported that the sensitivity and specificity of OCT for lipid-rich plaques were 90% to 94% and 90% to 92%, respectively (19). The fibrous cap generally presents high-intensity regions with low attenuation by OCT because the fibrous cap is composed mainly of collagen fibers and smooth muscle cells. On the basis of these features, OCT is a promising imaging modality for visualizing the morphological features of TCFAs.

However, there are some discrepancies between the incidence of TCFAs in OCT studies and histological studies. A previous OCT study reported that the incidence of TCFAs in patients with stable angina was 14.9% and the average number of lipid-rich plaques per patient was 1.9 ± 1.4 (20). In contrast, a 3-vessel histological study indicated that the average number of TCFAs was 0.46 ± 0.95 (21). Although the reasons for this discrepancy are unknown, they may relate to differences in patient populations. Another potential reason is that OCT may overestimate the incidence of TCFA in vivo. Because of the features of near-infrared light, the OCT signal is highly attenuated because of multiple scattering events in lipidic tissue (18). Therefore, other tissues could also be represented as signal-poor regions if they have similar light-scattering properties under OCT.

In accordance with our findings, a previous study showed that the accumulation of superficial foam cells can create a TCFA-like image even in the absence of an underlying necrotic core because of

FIGURE 3 Diagnostic Accuracy of IVUS-Derived TCFA-Like Image, OCT-Derived TCFA, and Both OCT- and IVUS-Defined TCFA

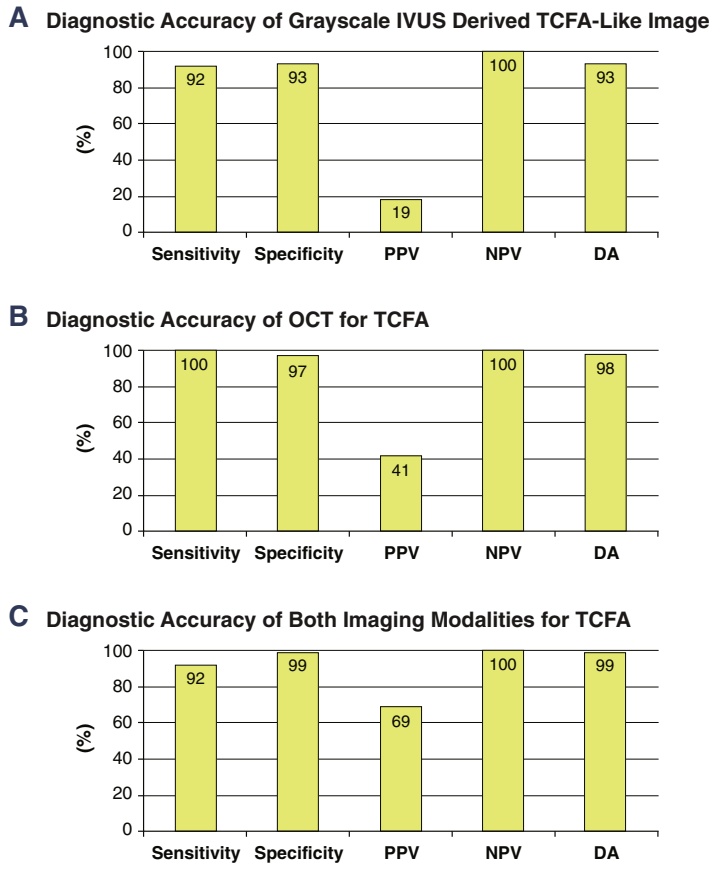

(A) Diagnostic accuracy of IVUS for TCFA-like image. **(B)** Diagnostic accuracy of OCT for TCFA. **(C)** Diagnostic accuracy of both IVUS- and OCT-defined TCFA. Abbreviations as in Figures 1 and 2.

FIGURE 4 False Positive Diagnoses by OCT for TCFA

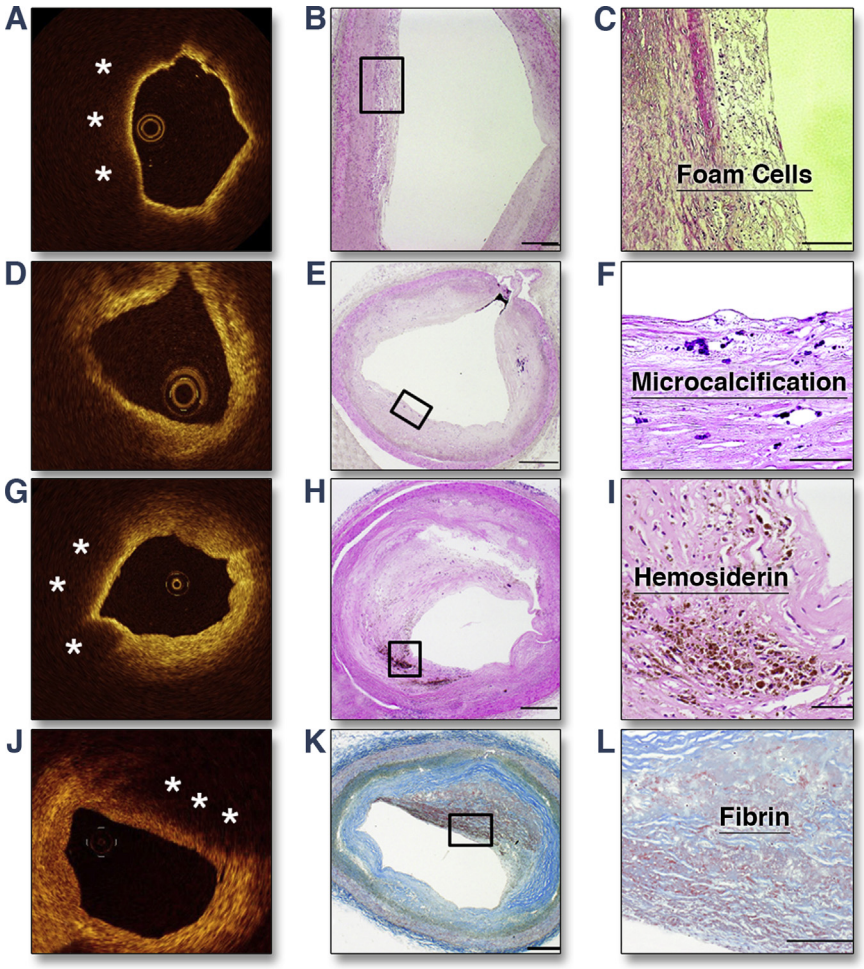

(A, D, G, and J) OCT images indicating a low-intensity area **(asterisks)** with an overlying signal-rich band. All lesions were diagnosed as TCFA by OCT. **(B, E, H, and K)** Large necrotic cores overlying a thin fibrous cap were not identified by corresponding histological images (scale bar = 500 μm). **(C)** A corresponding histological image from the same section of the lesion in **B** showed large amounts of foam cell accumulation on the luminal surface (hematoxylin-eosin stain, scale bar = 100 μm). **(F)** A histological image of the same cross section of the lesion in **E** revealed large amounts of microcalcification at the surface of fibrous intima (hematoxylin-eosin stain, scale bar = 50 μm). **(I)** A corresponding histological image from the same section of the lesion in **H** showed large amounts of hemosiderin accumulation on the luminal surface (hematoxylin-eosin stain, scale bar = 100 μm). **(L)** A corresponding cross-sectional histological image of the lesion in **K** showed an organized thrombus (Masson's trichrome, scale bar = 200 μm). Abbreviations as in Figures 1 and 2.

the presence of a strong scattering layer at the luminal surface with extensive underlying signal attenuation (22). In this ex vivo study, CD68-stained dense macrophage infiltration creates a highly scattering layer that casts a dark shadow on the tissue behind. This region appears as a TCFA. OCT signal analysis indicated that the macrophage layer is strongly scattering and rapidly attenuates the OCT beam. A recent ex vivo histological validation study of in-stent restenosis tissue showed that foam cell accumulation close to the luminal surface appears as a TCFA-like image (23). Similarly, another study reported that an organized thrombus also appeared as a high backscattering region with extensive OCT signal attenuation (23). OCT signal analysis indicated that OCT signal was significantly attenuated by fibrin because of the strong optical absorption of fibrin. The current study showed that the accumulation

FIGURE 5 A Representative Case of OCT- and IVUS-Defined TCFA

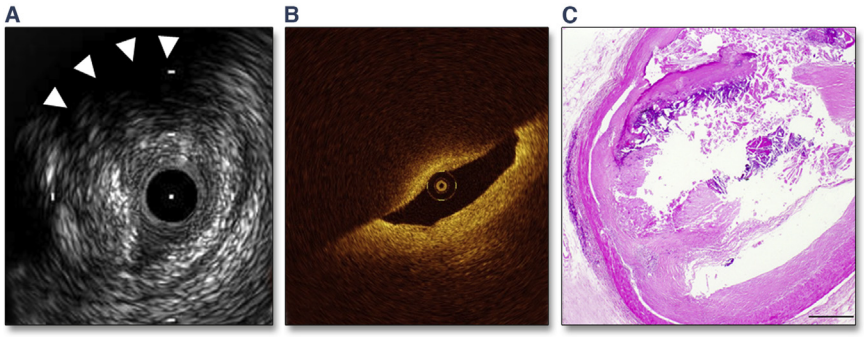

(A) Grayscale IVUS showing a plaque burden of 82% and a remodeling index of 1.31. Backward signal attenuation behind the plaque and without dense calcium was observed at 10 o'clock **(arrowheads)**. **(B)** A corresponding OCT image indicated signal-poor lesions with an overlying signal-rich band. The minimum fibrous cap thickness was 50 μm. **(C)** A corresponding histological image showing large necrotic cores covered by a thin (50-μm) fibrous cap (hematoxylin-eosin stain, scale bar = 500 μm). Abbreviations as in Figures 1 and 2.

of superficial hemosiderin also created a TCFA-like image even in the absence of an underlying necrotic core. Light signal is strongly attenuated by hemoglobin (a precursor of hemosiderin) due to absorption at light wavelengths around 1,000 nm. This is the reason why red blood cells need to be removed from the imaging field for OCT image acquisition. OCT signal might be highly attenuated by hemosiderin for the similar reason. The precise reason for creating a TCFA-like image of the deposition of microcalcification on the luminal surface is unclear. OCT light signal attenuation caused by multiple scattering may be a reason why this tissue appeared in the OCT as low-signal-intensity regions with diffuse borders. Because OCT measures the intensity of light returning from within a tissue, tissue having a higher heterogeneity of optical index of refraction, such as microcalcification deposition on the luminal surface, may exhibit stronger optical scattering (Figure 7). A previous study reported that the index of light refraction of calcium hydroxyapatite is higher than that of other tissues (24). The existence of these false positive examples might be a possible cause lowering a PPV of OCT for

FIGURE 6 Grayscale IVUS-Derived TCFA-Like Images

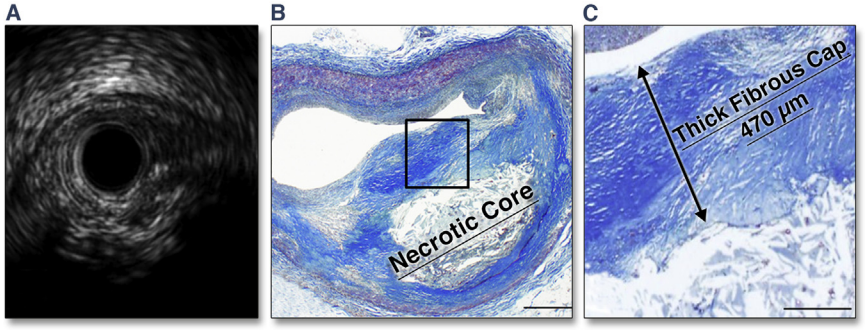

(A) Grayscale IVUS showing a plaque burden of 89% and a remodeling index of 1.22. Backward signal attenuation behind plaque without dense calcium indicates grayscale IVUS-derived TCFA-like images. **(B)** A corresponding histological image shows a fibroatheroma with large necrotic core overlying a thick fibrous cap (Masson's trichrome, scale bar = 500 μm). **(C)** The thick fibrous cap measured 470 μm (Masson's trichrome, scale bar = 200 μm). Abbreviations as in Figure 2.

FIGURE 7 A Representative Image for the Usefulness of Grayscale IVUS in Addition to OCT for the Diagnosis of TCFA

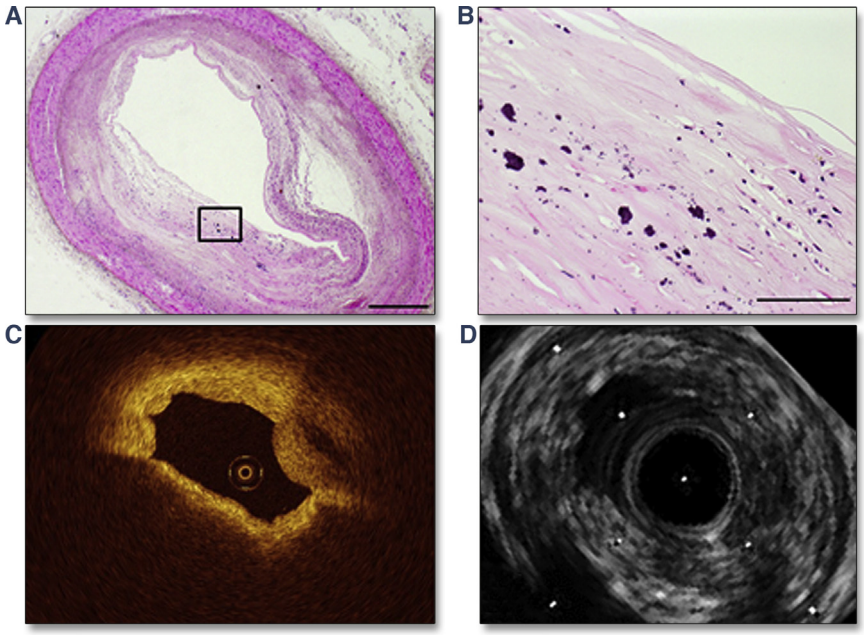

(A and B) The histological image showed fibrous plaque with large amounts of microcalcification on the luminal surface (hematoxylin-eosin stain, scale bar = 500 μm in **A** and 100 μm in **B**). **(C)** A corresponding OCT image showed a low-intensity area with a diffuse border overlying a high-intensity band. This plaque was diagnosed as TCFA by OCT imaging. **(D)** A corresponding IVUS image showed a plaque burden of 81% and a remodeling index of 0.91 without the presence of ultrasound attenuation and a lipid pool-like image. This plaque was not diagnosed as a grayscale IVUS-derived TCFA-like image. Accordingly, this plaque did not meet the criteria for TCFA when both IVUS and OCT criteria were required. Abbreviations as in Figures 1 and 2.

characterizing TCFAs using histology as a standard. Therefore, careful interpretation is required to identify TCFA by OCT, and longitudinal imaging with extension of the necrotic core proximal and distal to the lesion may be helpful.

In addition, the vessel remodeling status, which is one of the main findings for plaque vulnerability, cannot be evaluated by OCT because the penetration depth of OCT is limited to 1 to 2 mm. Because the tissue penetration ability of IVUS is markedly superior to that of OCT, the combined use of IVUS and OCT may help to identify vulnerable plaques. A recent study of human cadaver coronary suggested that almost all plaques with superficial echo attenuation indicated the presence of a fibroatheroma with an advanced necrotic core (25). Thus, the combined use of these complementary imaging modalities—grayscale IVUS and OCT—may result in more accurate identification of TCFA in clinical settings. In this regard an intravascular imaging catheter with dual grayscale IVUS and OCT capabilities has recently been developed and has already been tested in vitro, ex vivo, and in vivo (26).

STUDY LIMITATIONS. The present study has several limitations. First, we examined coronary arteries derived from autopsy in the hearts of patients following noncardiovascular death. The histological prevalence of TCFA was therefore low (2%). Although sensitivity and specificity are independent of prevalence, the PPV and NPV for OCT, IVUS, and their combination may have varied had the prevalence been higher. Second, a positional discrepancy in the evaluated cross sections among OCT, IVUS, and histological images may have influenced the results, although we took care to achieve optimal coregistration of OCT and IVUS images with histology. Third, the OCT and IVUS images of coronary arteries were taken from cadavers, obviously in the absence of cardiac motion. Cardiac motion artifacts may influence the images taken in vivo. Fourth, conventional grayscale IVUS was used in the current study. Radiofrequency IVUS combined with OCT may have

improved the diagnostic performance of IVUS (27). Fifth, to measure remodeling index, vessel area at the site with smallest lumen area was compared to that at the reference site. The sites with minimum lumen area and thinnest fibrous cap within plaques are not always identical. Sixth, lack of immunochemical staining to identify macrophages is an additional limitation. Finally, the statistical power to assess the diagnostic accuracy of TCFA was limited by the small number of histological TCFAs, and therefore, further investigations with larger cohorts are required to confirm the significance and applications of our findings.

CONCLUSIONS

In the present study, neither OCT nor IVUS were optimal to detect TCFA. The combined use of OCT and IVUS may improve TCFA detection accuracy in the clinical setting.

ACKNOWLEDGMENTS The authors thank the staff members from the Department of Surgical Pathology at Hyogo College of Medicine for their excellent assistance for the study.

REPRINT REQUESTS AND CORRESPONDENCE: Dr. Kenichi Fujii, Cardiovascular Division, Hyogo College of Medicine, 1-1 Mukogawa-cho, Nishinomiya, Hyogo 6638501, Japan. E-mail: kfujii@hyo-med.ac.jp.

PERSPECTIVES

COMPETENCY IN MEDICAL KNOWLEDGE: Neither optical coherence tomography nor IVUS were optimal to accurately identify coronary vulnerable plaques due to the existence of several false positive examples that have similar light and/or ultrasonic scattering properties. The combined use of these complementary imaging modalities may result in more accurate identification of vulnerable plaques in clinical settings.

TRANSLATIONAL OUTLOOK: Additional clinical studies are needed to validate what intracoronary imaging modalities could provide more accurate identification and characterization of vulnerable plaques to predict future cardiovascular event and mortality.

REFERENCES

1. Goldstein JA, Demetriou D, Grines CL, Pica M, Shoukfeh M, O'Neill WW. Multiple complex coronary plaques in patients with acute myocardial infarction. N Engl J Med 2000;343:915–22.

2. Virmani R, Kolodgie FD, Burke AP, Farb A, Schwartz SM. Lessons from sudden coronary death: a comprehensive morphological classification scheme for atherosclerotic lesions. Arterioscler Thromb Vasc Biol 2000;20:1262–75.

3. Fuster V, Stein B, Ambrose JA, Badimon L, Badimon JJ, Chesebro JH. Atherosclerotic plaque rupture and thrombosis. Evolving concepts. Circulation 1990;82:Ii47–59.

4. Yamagishi M, Terashima M, Awano K, et al. Morphology of vulnerable coronary plaque: insights from follow-up of patients examined by intravascular ultrasound before an acute coronary syndrome. J Am Coll Cardiol 2000;35:106–11.

5. Yamada R, Okura H, Kume T, et al. Histological characteristics of plaque with ultrasonic attenuation: a comparison between intravascular ultrasound and histology. J Cardiol 2007;50:223–8.

6. Kotani J, Mintz GS, Castagna MT, et al. Intravascular ultrasound analysis of infarct-related and non-infarct–related arteries in patients who presented with an acute myocardial infarction. Circulation 2003;107:2889–93.

7. Nissen SE, Yock P. Intravascular ultrasound: novel pathophysiological insights and current clinical applications. Circulation 2001;103:604–16.

8. Brezinski ME, Tearney GJ, Bouma BE, et al. Optical coherence tomography for optical biopsy. Properties and demonstration of vascular pathology. Circulation 1996;93:1206–13.

9. Jang IK, Tearney GJ, MacNeill B, et al. In vivo characterization of coronary atherosclerotic plaque by use of optical coherence tomography. Circulation 2005;111:1551–5.

10. Tearney GJ, Regar E, Akasaka T, et al. Consensus standards for acquisition, measurement, and reporting of intravascular optical coherence tomography studies: a report from the International Working Group for Intravascular Optical Coherence Tomography Standardization and Validation. J Am Coll Cardiol 2012;59:1058–72.

11. Fujii K, Kawasaki D, Masutani M, et al. OCT assessment of thin-cap fibroatheroma distribution in native coronary arteries. J Am Coll Cardiol Img 2010;3:168–75.

12. Mintz GS, Nissen SE, Anderson WD, et al. American College of Cardiology Clinical Expert Consensus Document on Standards for Acquisition, Measurement and Reporting of Intravascular Ultrasound Studies (IVUS). A report of the American College of Cardiology Task Force on Clinical Expert Consensus Documents. J Am Coll Cardiol 2001;37:1478–92.

13. Endo M, Hibi K, Shimizu T, et al. Impact of ultrasound attenuation and plaque rupture as detected by intravascular ultrasound on the incidence of no-reflow phenomenon after percutaneous coronary intervention in ST-segment elevation myocardial infarction. J Am Coll Cardiol Intv 2010;3:540–9.

14. Tanaka A, Kawarabayashi T, Nishibori Y, et al. No-reflow phenomenon and lesion morphology in patients with acute myocardial infarction. Circulation 2002;105:2148–52.

15. Nakamura M, Nishikawa H, Mukai S, et al. Impact of coronary artery remodeling on clinical presentation of coronary artery disease: an intravascular ultrasound study. J Am Coll Cardiol 2001;37:63–9.

16. Smits PC, Pasterkamp G, de Jaegere PP, de Feyter PJ, Borst C. Angioscopic complex lesions are predominantly compensatory enlarged: an angioscopy and intracoronary ultrasound study. Cardiovasc Res 1999;41:458–64.

17. Gronholdt ML. Ultrasound and lipoproteins as predictors of lipid-rich, rupture-prone plaques in the carotid artery. Arterioscler Thromb Vasc Biol 1999;19:2–13.

18. Allen TJ, Hall A, Dhillon AP, Owen JS, Beard PC. Spectroscopic photoacoustic imaging of lipid-rich plaques in the human aorta in the 740 to 1400 nm wavelength range. J Biomed Optics 2012;17:061209.

19. Yabushita H, Bouma BE, Houser SL, et al. Characterization of human atherosclerosis by optical coherence tomography. Circulation 2002;106:1640–5.

20. Kato K, Yonetsu T, Kim SJ, et al. Nonculprit plaques in patients with acute coronary syndromes have more vulnerable features compared with those with non-acute coronary syndromes: a 3-vessel optical coherence tomography study. Circ Cardiovasc Imaging 2012;5:433–40.

21. Cheruvu PK, Finn AV, Gardner C, et al. Frequency and distribution of thin-cap fibroatheroma and ruptured plaques in human coronary arteries: a pathologic study. J Am Coll Cardiol 2007;50:940–9.

22. van Soest G, Regar E, Goderie TP, et al. Pitfalls in plaque characterization by OCT: image artifacts in native coronary arteries. J Am Coll Cardiol Img 2011;4:810–3.

23. Nakano M, Vorpahl M, Otsuka F, et al. Ex vivo assessment of vascular response to coronary stents by optical frequency domain imaging. J Am Coll Cardiol Img 2012;5:71–82.

24. Cilingiroglu M, Oh JH, Sugunan B, et al. Detection of vulnerable plaque in a murine model of atherosclerosis with optical coherence tomography. Catheter Cardiovasc Interv 2006;67:915–23.

25. Pu J, Mintz GS, Biro S, et al. Insights into echo-attenuated plaques, echolucent plaques, and plaques with spotty calcification: novel findings from comparisons among intravascular ultrasound, near-infrared spectroscopy, and pathological histology in 2,294 human coronary artery segments. J Am Coll Cardiol 2014;63:2220–33.

26. Li BH, Leung AS, Soong A, et al. Hybrid intravascular ultrasound and optical coherence tomography catheter for imaging of coronary atherosclerosis. Catheter Cardiovasc Interv 2013;81:494–507.

27. Stone GW, Maehara A, Lansky AJ, et al. A prospective natural-history study of coronary atherosclerosis. New Engl J Med 2011;364:226–35.

KEY WORDS intravascular ultrasound, optical coherence tomography, vulnerable plaque